Balanced Carrier Transports of Electrons and Holes in Silole-Based Compounds−A Theoretical Study

Shiwei Yin, Yuanping Yi, Qingxu Li, Gui Yu, Yunqi Liu, and Zhigang Shuai*

Key Laboratory of Organic Solids, Beijing National Laboratory for Molecular Sciences, Institute of Chemistry, Chinese Academy of Sciences, 100080 Beijing, People's Republic of China

Received: December 14, 2005; In Final Form: March 15, 2006

By employing a diabatic model and a first-principle direct method, we have investigated the carrier transport properties of the highly efficient organic light-emitting materials 1,1,2,3,4,5-hexaphenylsilole (HPS) and 1-methyl-1,2,3,4,5-pentaphenylsilole (MPPS). The electronic coupling constants and reorganization energies are calculated for a wide variety of nearest-neighbor charge transfer pathways. The theoretical calculations show that (i) the electron mobility is very close to that of the hole, which indicates a balanced carrier transport in these materials, and (ii) the carrier mobilities for MPPS are larger than those for HPS. These results help explain the underlying microscopic mechanism for the high electroluminescence efficiency.

I. Introduction

Since the first discovery of an organic electroluminescent device by Tang and Van Slyke,[1] there has been considerable research interest in organic light-emitting diodes (OLEDs) both by academia and industry. Two important conditions are required to guarantee good performance of OLED devices: a high carrier geminate recombination rate and a high solid-state luminescence efficiency. The OLED external quantum efficiency can be expressed as $\eta_{EL} = r_{pair} r_s r_{PL} \alpha$. Here, r_{pair} is the proportion of injected carriers that form bound electron−hole pairs, r_s is the proportion of such electron−hole pairs that have a singlet spin and can therefore fluoresce, r_{PL} is the singlet exciton radiative decay (or photoluminescence) efficiency, and α is the optical outer coupling factor, which measures the proportion of generated photons that can escape the device (most of the generated photons are reflected at the interfaces and are reabsorbed by the materials). According to the anisotropic emission dipole model,[2,3] $\alpha = 1/n^2$, where n is the refractive index of the emissive medium. For instance, for $n = 1.5$, α is about 33%. According to spin statistics, r_s is limited to 25%, because, of the four microstates formed by two spin one-half particles (the injected electron and hole), one microstate is singlet and three are triplet. In pure organic systems, the triplet emission is forbidden. A major advance in the field was made by Forrest, Thompson, and co-workers,[4] who showed that incorporating heavy metals into organics can greatly increase the light-emitting efficiency, since the metal-induced spin−orbit coupling can result in triplet emission in addition to singlet emission. Recent progress also showed that, even for pure organic conjugated polymers, r_s can well exceed the 25% limit,[5] because the charge recombination processes are spin-dependent with, for conjugated polymers, the singlet exciton formation rate being much higher than the triplet exciton formation rate. As for the PL quantum efficiency (r_{PL}), it is known that solid-state effects usually quench luminescence either by intermolecular charge transfer or by energy transfer. However, our recent studies showed[6,7] that, in some cases, aggregation effects can enhance the photoluminescence. For instance, in siloles, the radiative decay is found to be slower than the radiationless process, with the latter being very much pronounced due to the facile rotation of the phenyl side groups. We showed that aggregation effects can, in this case, slow the radiationless process by hindering the side-group rotation and increase the proportion of radiative decay. In fact, the PL quantum efficiency of silole molecules in the solid state is far larger than that in solution, and the external quantum efficiencies of the silole-based molecule OLEDs are found to be 7−8%.[3,8]

In optimizing the proportion of free carriers that form geminate pairs, r_{pair}, a factor that is of utmost importance is that the injection and transport of electrons and holes be balanced. In an OLED device, rather than form a geminate pair, the electron or hole can either be trapped by defects or be absorbed by the electrodes to form a current. A balance transport between electron and hole can increase the recombination region. In this work, we are mostly interested in the carrier transport behaviors in silole-based OLED materials. We note that, in most organic material systems, the electron mobility is much smaller than the hole mobility, since, in either molecular crystals or conjugated polymers, the highest occupied band is usually wider than the unoccupied band.[9] The resulting unbalanced transport leads to loss of carriers during device operation and places an important limit on the OLED efficiency.

The silicon containing cyclic π-conjugated system silole (silacyclopentadiene) is a promising emissive material, due to its notable aggregation-enhanced emission[7] and high PL efficiency[10] in thin solid film. Siloles are believed to be an excellent electron transport material, because the presence of the silicon atom lowers the lowest unoccupied molecular orbital (LUMO) energy level relative to that of pure hydrocarbon molecules and this facilitates electron injection. The lowering of the LUMO has been ascribed to the interaction between the σ^* orbital of two exocyclic σ-bonds on the silole ring and the π^* orbital of the butadiene moiety.[4] Risko et al. utilized density functional theory (DFT) to study the electronic structure, including excited-state properties, vertical electron affinities, and reorganization energies as well as adiabatic electron affinities for silole-based molecules.[11] They found that the silole-based molecules have low-lying LUMOs and very large electron affinities, which leads to facile electron injection from metal electrodes.

* E-mail: zgshuai@iccas.ac.cn.

10.1021/jp057291o CCC: $33.50
Published on Web 05/13/2006

In this work, we apply a dimer model derived from the molecular crystal structure to study the transport behaviors of electrons and holes in silole-based materials. In contrast to most of the organic materials, we find that a balanced transport exists; namely, the electron and hole mobilities are close in value. We attribute the high OLED efficiency of siloles (7−8%) to the balanced carrier transport, in addition to the high solid-state PL efficiency.

II. Theoretical and Computational Methodology

Generally speaking, there are two extreme types of carrier motion in the solid state: (i) that of the coherent band model and (ii) that of the incoherent hopping model. In the band model, the carrier moves as a highly delocalized plane wave in an energy band with a relatively long mean free path ($\sim \mu$m). The interaction between the nearest-neighbor sites (charge transfer integral) is large compared with dynamic disorder, that is, the reorganization energy resulting from charge transfer from one molecule to another. This model is usually suitable for inorganic semiconductors where the interaction between different sites is through strong valence bonds and the room temperature mobility is far bigger than 1 $cm^2\ V^{-1}\ s^{-1}$. In the hopping model, the carrier is localized and moves by hopping from site to site, carrying a structural deformation with it. The basic characteristic of this model is that the lattice phonons are strongly coupled with the charge carrier, such that the wave momentum (k) that characterizes a band state is not conserved. The room temperature mobility for the hopping model is usually far smaller than 1 $cm^2\ V^{-1}\ s^{-1}$ and is proportional to $\exp(-E_a/kT)$, where E_a is an activation energy,[12] that is, the energy barrier that must be overcome to transfer a carrier to an adjacent site. For most organic molecular crystals, the interaction between different molecules is through a van der Waals potential and the electron coupling term (transfer integral t) is smaller than the reorganization energy. To the best of our knowledge, the largest mobility seen for amorphous siloles is about 2×10^{-4} $cm^2\ V^{-1}\ s^{-1}$,[13] which is far smaller than 1 $cm^2\ V^{-1}\ s^{-1}$. Thus, siloles fall in the hopping regime. In this model, the hopping rate can be described by Marcus theory via the following equation:[14]

$$k_{et} = \frac{4\pi^2}{h}\frac{1}{\sqrt{4\pi\lambda k_B T}} t^2 \exp\left\{-\frac{(\Delta G^0 + \lambda)^2}{4\lambda k_B T}\right\} \qquad (1)$$

Here, λ is the reorganization energy, ΔG^0 is the free energy difference between the initial and final site, and t is the charge transfer integral. For our case, where all sites are equivalent, ΔG^0 is zero. In this work, we do not consider the entropic contribution to the free energy, which is much less pronounced in the solid state than in liquid solvent. Thus, the charge transfer rate is determined by two important parameters: the electron transfer integral (t) and the reorganization energy (λ). λ contains the internal reorganization energy (λ_i) and the external polarization (λ_e). λ_i reflects the change in molecular geometry associated with going from the neutral to the ionized state, or vice versa. λ_e describes the change in electronic polarization of the surrounding molecules. This value is difficult to evaluate theoretically and consists of one of the challenges for theoretical chemistry.[15] For organic solids and weak polar media, the medium contribution to the relaxation energy is on the order of a few tenths of an electronvolt.[16] Once the transfer rate is obtained, the carrier mobility can be expressed as

$$\mu = \frac{v}{F} = \frac{\frac{a}{\Delta t}}{F} = \frac{a k_{et}}{F} \qquad (2)$$

where a is the hopping distance between nearest sites, F is the electric-field strength, and the transfer time (Δt) is inversely proportional to k_{et}.

We investigate two silole-based molecular materials, 1,1,2,3,4,5-hexaphenylsilole (HPS) and 1-methyl-1,2,3,4,5-pentaphenylsilole (MPPS), shown in Figure 1. We will mainly focus on

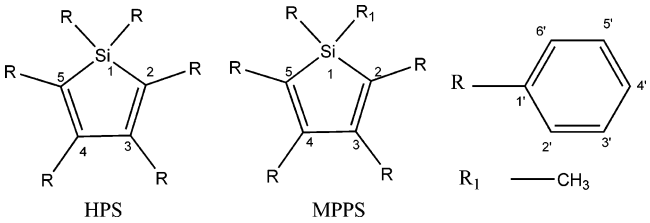

Figure 1. Chemical structure of HPS (left) and MPPS (right).

calculating charge transfer integrals for different transfer pathways. To evaluate the electronic interaction using a dimer model, we need to know the relative position of relevant nearest-neighbor pairs of molecules in the material. In OLED devices, the organic semiconductor materials usually form amorphous structures. However, the amorphous material can be considered as having short-range-ordered aggregation, with structures that are locally close to those seen in the crystalline state. Indeed, Lin et al.[17] have adopted a dimer model derived from molecular crystal structure data and applied Koopmans' theorem (indirect method) as well as the direct method to evaluate the electronic couplings for a prototype of Alq_3-based OLED materials. Their calculations predict that the electron mobility is more than 2 orders of magnitude larger than the hole mobility, which is in good agreement with the experimental finding that Alq_3 is an excellent electron transport material. Here, we use the single crystal structures of HPS[18] and MPPS[6] (Figure 2) to generate a wide variety of possible intermolecular hopping pathways. The construction of these pathways will be illustrated using the HPS crystal as an example. The crystal structure of HPS belongs to the triclinic system with space group $P\bar{1}$. The unit-cell lengths OA, OB, and OC are 9.527, 10.043, and 16.308 Å, respectively. The unit cell contains two inequivalent molecules. We label the molecule with the silicon atom coordinated at (0.39, 0.397, 0.315) as molecule A and the other as molecule B. We take the primitive cell centered at (0, 0, 0) as the origin. There are two kinds of dimers: A−A and A−B. The first occurs only between cells, while the latter occurs both within and between cells. In this way, we can construct a large number of transport pathways (see Tables 1 and 2).

Once a transport pathway is defined, the electronic coupling can be calculated through the diabatic model. The two diabatic states correspond to the carrier localized on the electron donating and accepting molecules, respectively. The electronic coupling can be obtained either by Koopmans' theorem at the Hartree−Fock mean-field level (indirect method) or by the direct method. In the former case, the charge transfer integral is equal to the energy splitting between the highest occupied molecular orbital (HOMO) and HOMO-1 (for hole carrier) or between the LUMO and LUMO+1 (for electron carrier) of the dimer. Brédas et al. have extensively investigated the intermolecular couplings including the effects of relative orientation, separation, and substitution for prototypical conjugated systems such as polyenes, stilbene, and discotic hexabenzocoronene using a semiem-

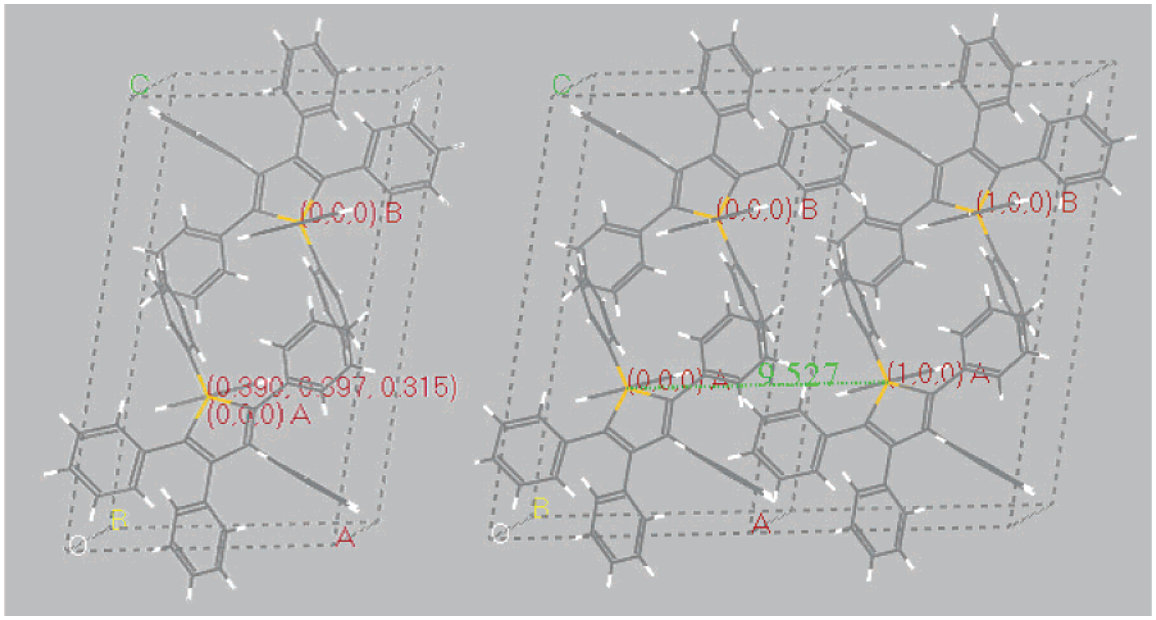

Figure 2. Crystal structure of HPS. The left panel is the primitive cell, numbered as (0,0,0), containing two silole molecules, (0,0,0)-A and (0,0,0)-B. The right panel shows two linked unit cells, numbered as (0,0,0) and (1,0,0).

TABLE 1: Charge Transfer Integrals (t_h for Hole and t_e for Electron) between Molecule A in the HPS Crystal (0,0,0) Unit Cell and the Other Most Possible Adjacent Molecules

pathway	A−A	A−A	A−A	A−B	A−B	A−B	A−B	A−B	A−B	A−B	A−B
channel	I	II	III	IV	V	VI	VII	VIII	IX	X	XI
cartner	(±1,0,0)	(0,±1,0)	(0,0,±1)	(0,0,0)	(−1,0,0)	(0,−1,0)	(0,0,−1)	(−1,−1,0)	(−1,0,−1)	(0,−1,−1)	(−1,−1,−1)
Si−Si distance/Å	9.53	10.04	16.31	7.20	8.70	8.78	9.99	12.40	13.18	13.85	18.03
t_h/meV	0.79	0.46	0.03	17.69	0.08	2.39	2.26	0.05	4.87	2.39	0.03
t_e/meV	6.61	1.17	0.03	12.82	1.25	14.10	1.85	0.14	4.41	12.05	0.19

TABLE 2: Charge Transfer Integrals (t_h for Hole and t_e for Electron) between Molecule A in the MPPS Crystal (0,0,0) Unit Cell and the Other Most Possible Adjacent Molecules

pathway	I (A−A)	I (A−A)	I (A−A)	II (A−B)	II (A−B)	II (A−B)	II (A−B)	II (A−B)	II (A−B)	II (A−B)	II (A−B)
channel	I	II	III	IV	V	VI	VII	VIII	IX	X	XI
partner	(±1,0,0)	(0,±1,0)	(0,0,±1)	(0,0,0)	(−1,0,0)	(0,−1,0)	(0,0,−1)	(−1,−1,0)	(−1,0,−1)	(0,−1,−1)	(−1,−1,−1)
Si−Si distance/Å	10.19	11.27	11.98	13.72	7.48	15.33	10.66	10.42	6.10	12.88 9.76	
t_h/meV	7.70	1.09	4.54	0.03	33.47	5.82	0.54	4.38	2.10	0.98	3.10
t_e/meV	15.08	0.54	1.39	0.08	43.97	4.08	0.49	7.95	18.04	1.74	1.80

pirical indirect approach.[19] Yang et al. have applied the same approach to investigate the coupling between carbon nanotubes.[20] However, this scheme sometimes fails, when the HOMO and HOMO-1 or LUMO and LUMO+1 are not simple linear combinations of the HOMOs or LUMOs of the charge-localized isolated molecules.[21]

In modeling scanning tunneling microscopy, Fujita, Nakai, and Nakatsuji have worked out a straightforward direct scheme to obtain the electronic coupling term,[22] which does not make assumptions regarding the nature of the frontier orbitals of the molecular pair. Later, Troisi and Orlandi applied this approach to calculate charge transfer couplings in DNA and obtained quite satisfactory results in comparison with experiments.[23] This formalism has also been employed to investigate the spin-dependent exciton formation rates in polymer electroluminescence.[5b,24] In this paper, we adopt this direct approach to investigate charge transport properties in siloles. The electronic coupling in this scheme can be written as

$$t_{e/h} = \langle \phi^{0,site1}_{LUMO/HOMO} | F^0 | \phi^{0,site2}_{LUMO/HOMO} \rangle = \langle \phi^{0,site1}_{LUMO/HOMO} | h_{core} | \phi^{0,site2}_{LUMO/HOMO} \rangle + \sum_{l(occ)} (\langle \phi^{0,site1}_{LUMO/HOMO} \phi_l^0 | \phi^{0,site2}_{LUMO/HOMO} \phi_l^0 \rangle - \langle \phi^{0,site1}_{LUMO/HOMO} \phi^{0,site2}_{LUMO/HOMO} | \phi_l^0 \phi_l^0 \rangle) \quad (3)$$

where $t_{e/h}$ is the charge transfer coupling integral for the electron/hole and $\phi^{0,site1}_{LUMO/HOMO}$ and $\phi^{0,site2}_{LUMO/HOMO}$ represent the LUMOs/HOMOs of the two adjacent molecules 1 and 2 when no intermolecular interaction is presented. F^0 is the Fock operator for the dimer for a fixed pathway, and the suffix zero indicates that the molecular orbitals appearing in the operator (the density matrix, for instance) are unperturbed. The summation over l includes all of the occupied levels for both sites and represents the Coulomb and exchange interactions between the transferred electron/hole and the whole system. It has been shown that the exchange term can contribute to the spin dependence of the charge recombination rates in exciton formation.[5b] The non-interacting molecular orbitals of the two individual molecules are calculated separately by the standard self-consistent-field (SCF) procedure. These non-interacting orbitals are used to construct the dimer Fock matrix as well as the two-electron integrals in eq 3. More specifically, the non-interacting orbitals and associated density matrix are used in evaluating the Fock matrix of the dimer structure. All of the calculations are performed with the Gaussian 03 package[25] at the Hartree−Fock/6-31G(d) level. We also calculated the transfer integrals using the DFT/B3LYP method and found that DFT and HF give very similar results for the 6-31G(d) basis set, a fact already pointed out by Troisi et al.[23a]

TABLE 3: Interatomic Distances (in Å) between the Partners for HPS and MPPS

channel	Si1−Si1	C2−C2	C5−C5	C3−C3	C4−C4
HPS−IV	7.61	9.63	9.63	11.74	11.74
HPS−VI	8.78	9.16	9.16	10.26	10.26
MPPS−V	7.48	6.71	6.71	6.86	6.86
MPPS−IX	6.10	8.48	8.48	10.82	10.82

III. Results and Discussion

On the basis of the crystal structures of HPS and MPPS, we can identify 11 distinct nearest-neighbor hopping pathways. Using the method described above in eq 3, the corresponding coupling integrals were calculated for both the electron and hole, and these are presented in Table 1 for HPS and Table 2 for MPPS. It is interesting to note the following points:

(i) For both HPS and MPPS, the charge transfer integrals for the electron are very close to those of the hole. For instance, for MPPS, the dominant pathway is channel V, with $t_h = 33.47$ meV and $t_e = 43.97$ meV, respectively, while, for HPS, t_h and t_e are 17.69 and 12.82 meV, respectively, for channel IV. Although the former is larger than the latter, in HPS, three channels exist with t_e larger than 10 meV and only one for t_h.

(ii) The largest transfer integrals for MPPS (channel V) are notably larger than those for HPS (channel IV), indicating that the charge carrier mobilities in MPPS are larger than those in HPS. In fact, for both materials, the channels with the largest transfer integrals correspond to a shifted (almost parallel) cofacial arrangement between the silacycles of the dimer. We give in Table 3 some interatom distances of the partners for selected channels for comparison. Specifically, we find that the intercarbon distances in MPPS-channel V are around 6.7−6.9 Å, while, for HPS (channel IV), they are 9.6−11.7 Å. Apparently, the phenyl group (R_1, see Figure 1) presents larger steric hindrance than the methyl group such that MPPS has greater $\pi-\pi$ overlap.

(iii) In both HPS and MPPS, there exist channels through which the electron transfer is much larger than that for the hole, for instance, channel VI and channel X in HPS (Table 1) and channel IX in MPPS (Table 2). This can be explained by the charge distributions of the corresponding frontier orbitals. We first look at the HOMO and LUMO of HPS (Figure 3). Here, we find that the LUMO wave function is mainly localized on the silole ring, especially on the 2-, 1-, and 5-positions. There is also considerable electron density on the 1′-position of the silicon exocyclic aryl ring, which is due to interaction between the σ^* orbitals of the two exocyclic σ orbitals on the ring silicon and the π^* orbital of the butadiene moiety.[11,26] The HOMO is primarily located on the C2−C3 and C4−C5 double bonds in the silole ring as well as on the 2- and 5-positions in the aryl rings. In the configuration of channel VI (Figure 4), the distances between silole rings at the 1-, 2-, and 5-positions of the (0,0,0) A molecule and the (0,−1,0) B molecule are smaller than those at the 3- and 4-positions, which eventually make the intermolecular overlap for LUMOs larger than that for HOMOs.

LDA−DFT calculations were used to estimate the reorganization energies, based on the relaxation energies of the anion and the cation of MPPS and HPS. The internal reorganization energy (λ_i) is 0.34 eV for the electron of MPPS. (Allowing the

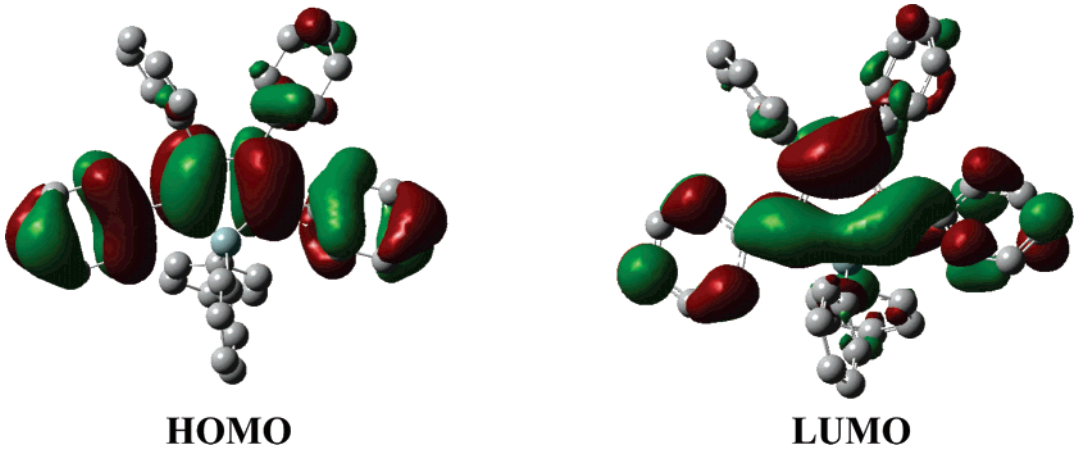

Figure 3. HOMO and LUMO of an HPS molecule.

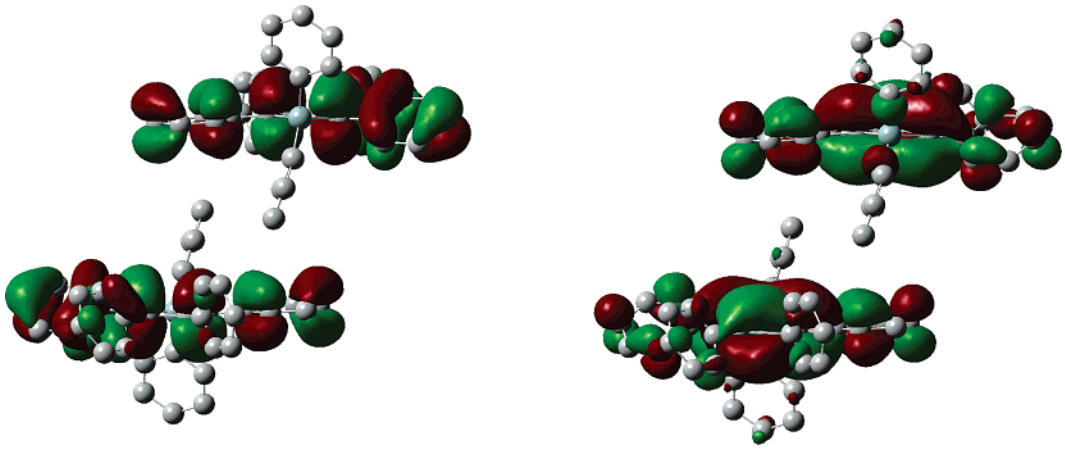

Figure 4. HPS dimer structure, including frontier molecular orbitals of (0,0,0) A(down) and (0,−1,0) B(up) molecules. The left panel shows the HOMOs, and the right panel shows the LUMOs.

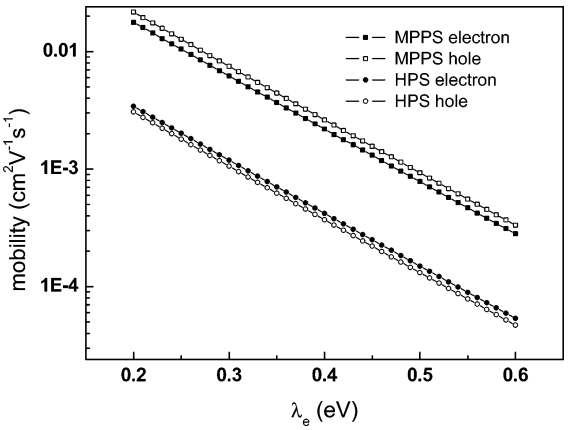

Figure 5. Theoretical estimation of the room temperature carrier mobilities for MPPS and HPS for the most favored transport channel, with an applied electric field of $F = 10^6$ V/cm.

anion to relax from the structure of the neutral molecule to that of the anion gives 0.18 eV, and allowing the neutral molecule to relax from the structure of the anion to that of the neutral gives 0.16 eV. Their sum gives the total internal reorganization energy, $0.18 + 0.16 = 0.34$ eV.) λ_i is 0.27 eV ($=0.14 + 0.13$) for the hole of MPPS. For HPS, the internal reorganization energies are 0.32 eV for the electron and 0.27 eV for the hole. For both MPPS and HPS, the reorganization energy of the hole is slightly smaller than that of the electron. On the other hand, we observed above that more transport channels exist for electrons than for holes. Globally, we can conclude that the carrier transport mobilities in siloles are balanced.

To have a rough estimate on the intermolecular charge transfer rate and the carrier mobility according to eqs 1 and 2, we assume the external reorganization energy (λ_e) is in the range 0.2−0.6 eV.[27] We take the largest charge transfer rates (channel IV for both HPS and MPPS) for eq 1, which give k_{et} in the range 10^9−10^{11} s^{-1} at $T = 300$ K. The resulting room temperature mobilities are plotted in Figure 5 for an electric-field strength of $F = 10^6$ V/cm, which is a typical value for an operating OLED device. The theoretical estimates are in the range 10^{-4}−10^{-2} cm^2 V^{-1} s^{-1}, the lower limit of which is in agreement with the experimental values of $\sim 10^{-4}$ cm^2 V^{-1} s^{-1}.[13] Note that the theoretical values are based on taking the most favorable transport intermolecular channel. On average, the mobility should be lower than this one.

It should also be noted that a number of effects are omitted in the above calculations. Thermal motions will lead to fluctuations in the intermolecular distances that can alter the charge transfer rates. Such fluctuations may influence some pathways more than others. As mentioned above, the effects of electronic polarization in the surrounding molecules are also ignored. Yaron and co-workers showed that such effects can alter the effective mass of the electron and hole[28] or, equivalently, add an additional contribution to the external reorganization energy. This issue deserves further investigation; however, we note that since the electronic polarization developed around a positive charge is similar to that developed around a negative charge,[28] this contribution is expected to have roughly equal effects on the electron and hole mobilities.

IV. Conclusion

This work used the crystal structures of HPS and MPPS to identify relevant charge transport pathways between adjacent molecules in these materials. A first-principles direct method, within the diabatic model, was then used to calculate the corresponding electronic couplings for these pathways. The resulting charge transfer integrals for the electron and hole were found to have very similar values. In addition, the reorganization energies associated with electron and hole transport were found to be very similar. This leads to the conclusion that, in both HPS and MPPS, the mobility of the electron is almost equal to that of the hole. We believe this balanced transport behavior is another important reason for the high electroluminescence efficiency achieved in the devices (the other reason being that aggregation enhances emission). We also find that the carrier mobilities in MPPS are larger than those in HPS. Finally, the estimated carrier mobilities are in good agreement with the experimental measurements.

Acknowledgment. The authors are grateful to Professor David Yaron for his careful, thorough, and critical readings of the manuscript. This work is supported by the Ministry of Science and Technology in China (973 program, Grant No. 2002CB613400) and National Science Foundation of China (Grant Nos. 20433070, 10425420, 90301001, and 20420150034). It is also supported by the Supercomputing Center of the Chinese Academy of Sciences.

References and Notes

(1) Tang, C. W.; Van Slyke, S. A. *Appl. Phys. Lett.* **1987**, *51*, 913.

(2) Kim, J. S.; Ho, P. K.; Greenham, N. C.; Friend, R. H. *J. Appl. Phys.* **2000**, *88*, 1073.

(3) Chen, H. Y.; Lam, Y. W.; Luo, J. D.; Ho, Y. L.; Tang, B. Z.; Zhu, D. B.; Wong, M.; Kwok, H. S. *Appl. Phys. Lett.* **2002**, *81*, 574.

(4) Baldo, M. A.; O'Brien, D. F.; You, Y.; Shoustikov, A.; Sibley, S.; Thompson, M. E. Forrest, S. R. *Nature (London)* **1998**, *395*, 151. Baldo, M. A.; Lamansky, S.; Burrows, P. E.; Thompson, M. E.; Forrest, S. R. *Appl. Phys. Lett.* **1999**, *75*, 4. Baldo, M. A; Thompson, M. E.; Forrest, S. R. *Nature (London)* **2000**, *750*, 403.

(5) (a) Cao, Y.; Parker, I. D.; Yu, G.; Zhang, C.; Heeger, A. J. *Nature (London)* **1999**, *414*, 397. (b) Shuai, Z.; Beljonne, D.; Silbey, R. J.; Brédas, J. L. *Phys. Rev. Lett.* **2000**, *84*, 131. (c) Wohlgenannt, M.; Tandon, K.; Mazumdar, S.; Ramasesha, S.; Vardeny, Z. V. *Nature (London)* **2001**, *494*, 409. (d) Karabunarliev, S.; Bittner, E. *Phys. Rev. Lett.* **2003**, *90*, 057402. (e) Yin, S. W.; Chen, L. P.; Xuan, P. F.; Chen, K. Q.; Shuai, Z. *J. Phys. Chem. B* **2004**, *108*, 9608. (f) Beljonne, D.; Ye, A.; Shuai, Z.; Brédas, J. L. *Adv. Funct. Mater.* **2004**, *14*, 684.

(6) Yu, G.; Yin, S. W.; Liu, Y. Q.; Chen, J. S.; Xu, X. J.; Sun, X. B.; Ma, D. G.; Zhan, X. W.; Peng, Q.; Shuai, Z.; Tang, B. Z.; Zhu, D. B.; Fang, W. H.; Luo, Y. *J. Am. Chem. Soc.* **2005**, *127*, 6335.

(7) (a) Luo, J. D.; Xie, Z.; Lam, J. W. Y.; Cheng, L.; Chen, H.; Qiu, C.; Kwok, H. S.; Zhan, X.; Liu, Y.; Zhu, D.; Tang, B. Z. *Chem. Commun.* **2001**, *18*, 1740. (b) Tang, B. Z.; Zhan, X.; Yu, G.; Lee, P. P. S.; Liu, Y.; Zhu, D. *J. Mater. Chem.* **2001**, *11*, 2874.

(8) Chen, J. W.; Xie, Z. L.; Lam, J. W. Y.; Law, C. C. W.; Zhu, D. B.; Tang, B. Z. *Macromolecules* **2003**, *36*, 1108.

(9) André, J. M.; Delhalle, J.; Brédas, J. L. *Quantum Chemistry Aided Design of Organic Polymers*; World Scientific Publishing Co. Pte. Ltd.: Singapore, 1991.

(10) (a) Palilis, L. C.; Makinen, A. J.; Uchida, M.; Kafafi, Z. H. *Appl. Phys. Lett.* **2003**, *82*, 2209. (b) Murata, H.; Kafafi, Z. H. *Appl. Phys. Lett.* **2002**, *80*, 189.

(11) (a) Risko, C.; Kushto, G. P.; Kafafi, Z. H.; Brédas, J. L. *J. Chem. Phys.* **2004**, *121*, 9031. (b) Risko, C.; Zojer, E.; Brocorens, P.; Marder, S. R.; Brédas, J. L. *Chem. Phys.* **2005**, *313*, 151.

(12) Pope, M.; Swenberg, C. *Electronic processes in organic crystals and polymers*, 2nd ed.; Oxford University Press: New York, 1999.

(13) Murata, H.; Malliaras, G. G.; Uchida, M.; Shen, Y.; Kafafi, Z. H. *Chem. Phys. Lett.* **2001**, *339*, 161.

(14) (a) Marcus, R. A. *Rev. Mod. Phys.* **1993**, *65*, 599. (b) Brédas, J. L.; Calbert, J. P.; da Silva Filho, D. A.; Cornil, J. *Proc. Natl. Acad. Sci. U.S.A.* **2002**, *99*, 5804.

(15) (a) Soos, Z. G.; Tsiper, E. V.; Painelli, A. *J. Lumin.* **2004**, *110*, 332. (b) Tsiper, E. V.; Soos, Z. G. *Phys. Rev. B* **2003**, *68*, 085301. (c) Tsiper, E. V.; Soos, Z. G.; Gao, W.; Kahn, A. *Chem. Phys. Lett.* **2002**, *360*, 47.

(16) Beljonne, D.; Ye, A. J.; Shuai, Z. G.; Brédas, J. L. *Adv. Funct. Mater.* **2004**, *14*, 684.

(17) Lin, B. C.; Cheng, C. P.; You, Z. Q.; Hsu, C. P. *J. Am. Chem. Soc.* **2005**, *127*, 66.

(18) Chen, J. W.; Law, C. C. W.; Lam, J. W. Y.; Dong, Y. P.; Lo, S. M. F.; Williams, I. D.; Zhu, D. B.; Tang, B. Z. *Chem. Mater.* **2003**, *15*, 1535.

(19) Brédas, J. L.; Beljonne, D.; Coropceanu, V.; Cornil, J. *Chem. Rev.* **2004**, *104*, 4971.

(20) Yang, X.; Chen, L. P.; Shuai, Z.; Liu, Y. Q.; Zhu, D. B. *Adv. Funct. Mater*. **2004**, *14*, 289.

(21) Lu, S. Z.; Li, X. Y.; Liu, J. F. *J. Phys. Chem. A* **2004**, *108*, 4125.

(22) Fujita, T.; Nakai, H.; Nakatsuji, H. *J. Chem. Phys.* **1996**, *104*, 2410.

(23) (a) Troisi, A.; Orlandi, G. *Chem. Phys. Lett.* **2001**, *344*, 509. (b) Orlandi, G.; Troisi, A.; Zerbetto, F. *J. Am. Chem. Soc.* **1999**, *121*, 5392.

(24) Ye, A.; Shuai, Z.; Brédas, J. L. *Phys. Rev. B* **2002**, *65*, 045208.

(25) Frisch, M. J.; et al. *Gaussian 03*, revision A.1; Gaussian, Inc.: Pittsburgh, PA, 2003.

(26) Tamao, K.; Uchida, M.; Izumizawa, T.; Furukawa, K.; Yamaguchi, S. *J. Am. Chem. Soc.* **1996**, *118*, 11974.

(27) Lemeur, V.; Steel, M.; Beljonne, D.; Brédas, J. L.; Cornil, J. *J. Am. Chem. Soc.* **2005**, *127*, 6077.

(28) Moore, E. E.; Gherman, B.; Yaron, D. *J. Chem. Phys.* **1996**, *106*, 4216. Moore, E. E.; Yaron D. *J. Chem. Phys.* **1998**, *109*, 6147. Yaron, D.; Moore, E. E.; Shuai, Z.; Brédas, J. L. *J. Chem. Phys.* **1998**, 108, 7451.